

# Edge Modes in the Intermediate- $D$ and Large- $D$ Phases of the $S = 2$ Quantum Spin Chain with $XXZ$ and On-Site Anisotropies

Kiyomi Okamoto<sup>1\*</sup>, Takashi Tonegawa<sup>2,3</sup>, Tôru Sakai<sup>4,5</sup>, and Makoto Kaburagi<sup>2</sup>

<sup>1</sup>*Department of Physics, Tokyo Institute of Technology, Tokyo 152-8551, Japan*

<sup>2</sup>*Professor Emeritus, Kobe University, Kobe 657-8501, Japan*

<sup>3</sup>*Department of Physical Science, School of Science, Osaka Prefecture University, Sakai 599-8531, Japan*

<sup>4</sup>*Japan Atomic Energy Agency, SPring-8, Hyogo 679-5148, Japan*

<sup>5</sup>*Graduate School of Material Science, University of Hyogo, Hyogo 678-1297, Japan*

We investigate the edge modes at  $T = 0$  in the intermediate- $D$  (ID) phase and the large- $D$  (LD) phase of the  $S = 2$  quantum spin chain with the  $XXZ$  anisotropy and the generalized on-site anisotropies by use of the DMRG. There exists a gapless edge mode in the ID phase, while no gapless edge mode in the LD phase. These results are consistent with the physical pictures of these phases. We also show the ground-state phase diagrams obtained by use of the exact diagonalization and the level spectroscopy analysis.

**KEYWORDS:** quantum spin chain models, quantum phase transitions, critical phenomena, DMRG, edge modes

## 1. Introduction

In these years quantum spin chains have been attracting a great deal of attention because rich physics is involved in spite of their apparent simplicity. The most striking example is the existence of the Haldane phase [1, 2] in the  $S = 1$  quantum spin chain only with nearest-neighbor (nn) isotropic interaction.

Very recently we [3–5] have investigated the  $S = 2$  quantum spin chain with the  $XXZ$  and on-site anisotropies described by

$$\mathcal{H} = \sum_j (S_j^x S_{j+1}^x + S_j^y S_{j+1}^y + \Delta S_j^z S_{j+1}^z) + D_2 \sum_j (S_j^z)^2, \quad (1)$$

where  $S_j^\mu$  ( $\mu = x, y, z$ ) denotes the  $\mu$ -component of the  $S = 2$  spin operator at the  $j$ -th site. The quantity  $\Delta$  represents the  $XXZ$  anisotropy parameter of the nn interaction, and  $D_2$  the on-site anisotropy parameter. The history of the works on the above model as of 2011 is summarized in [3].

We have obtained the phase diagram Fig.1 on the  $\Delta - D_2$  plane by use of the exact diagonalization (ED) and the level spectroscopy (LS) analysis [6–9] as well as the phenomenological renormalization group (PRG) analysis [10]. For simplicity we have restricted ourselves to the case where  $\Delta \geq 0$  and  $D_2 \geq 0$ . In this phase diagram there are four phases: the XY1 phase, the intermediate- $D$  (ID) phase, Haldane/large- $D$  (H/LD) phase and the Néel phase. The XY1 state is gapless and characterized by the power decay of the spin correlation function  $G_{\perp 1}(r) \equiv \langle S_1^+ S_r^- \rangle$ . The Haldane, ID and LD states are

---

\*E-mail address: kokamoto@phys.titech.ac.jp

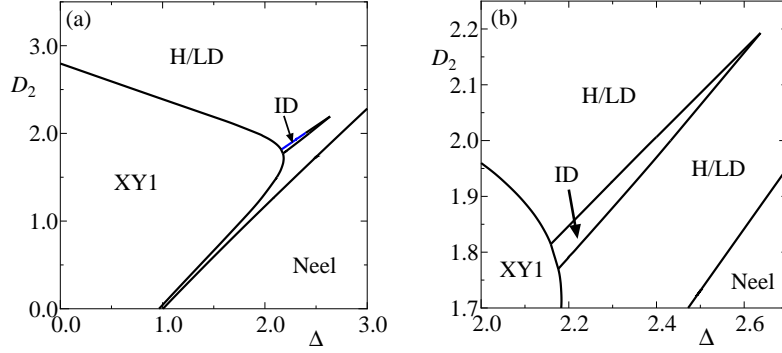


**Fig. 1.** Phase diagram of Hamiltonian (1) [3–5]. We have restricted ourselves to the case of  $\Delta \geq 0$  and  $D_2 \geq 0$ .

gapful and their valence bond solid (VBS) pictures are shown in Fig.2(a)-(c). The remarkable natures of this phase diagram are as follows: (A) there exists the ID phase which was predicted by Oshikawa about twenty years ago [11]; (B) the Haldane state and the LD state belong to the same phase which is called the H/LD phase. At a glance, the Haldane state and the LD state differ from each other. The reason why these two states are essentially the same is explained in Fig.2(d)-(f). The H/LD state is the four-spin cluster state, both limits of which are interpreted as the Haldane state and the LD state, respectively. Very similar situations are found in the  $S = 1$  chain with the on-site anisotropy and the bond alternation [12], and in the  $S = 1$  two-leg ladder [13].

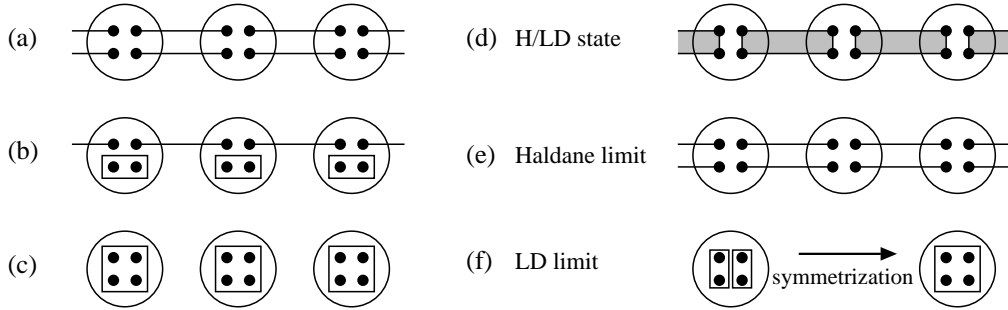


**Fig. 2.** VBS pictures for (a) the Haldane state, (b) the ID state and (c) the LD state. Big circles denote  $S = 2$  spins and dots  $S = 1/2$  spins. Solid lines represent valence bonds (singlet pairs of two  $S = 1/2$  spins,  $(1/\sqrt{2})(\uparrow\downarrow - \downarrow\uparrow)$ ). Two  $S = 1/2$  spins in rectangles are in  $(S_{\text{tot}}, S_{\text{tot}}^z) = (1, 0)$  state and similarly four  $S = 1/2$  spins in squares are in  $(S_{\text{tot}}, S_{\text{tot}}^z) = (2, 0)$  state. We show a VBS picture of the H/LD state in (d), where the shaded rectangles denote four-spin clusters. The Haldane state (e) and the LD state (f) are interpreted as the limiting cases of the four-spin cluster state.

Slightly after our works [3–5], Tzeng [14] confirmed our results by use of the density matrix renormalization group (DMRG) and the LS analysis. He used the parity DMRG because the classification of the eigenstates by the parity is essential for the LS analysis of the numerical data. Kjäll et al. [15] also investigated this model by use of the DMRG based on the matrix-product states to obtain the same conclusion as ours for (B) and slightly different conclusion from ours for (A). Namely, they claimed that the ID phase does not exist on the  $\Delta - D_2$  plane and very small  $D_4$  term (see eq.(2) and later) with  $D_4 > 0$  is necessary to realize the ID phase, although they could not completely rule out the possibility of the existence of the ID phase when  $D_4 = 0$ . We think that the difference

between our and their conclusions for (A) is not a serious problem. Since the edge of the ID phase in the  $\Delta - D_2 - D_4$  space near  $D_4 = 0$  may be very sharp, it is exceedingly difficult to numerically determine whether this sharp edge reaches the  $D_4 = 0$  plane or not.

In the  $S = 1$  chain problem, the edge modes under the open boundary condition (OBC) are very important to elucidate and characterize the nature of the Haldane state. In this paper, we investigate the edge modes of the H/LD state and the ID state. However, since the region of the ID phase on the  $\Delta - D_2$  plane, if exists, is very narrow as can be seen from Fig.1, it may be extremely difficult to obtain clear results on the edge modes. Thus, we modify the Hamiltonian into

$$\mathcal{H} = \sum_j (S_j^x S_{j+1}^x + S_j^y S_{j+1}^y + \Delta S_j^z S_{j+1}^z) + D_2 \sum_j (S_j^z)^2 + D_4 \sum_j (S_j^z)^4, \quad (2)$$

by introducing the  $D_4$  term to expand the region of the ID phase.

## 2. Phase Diagram

We mainly investigate two cases; the  $D_2 = -D_4$  case and the  $D_2 = 0$  case. The phase diagrams are shown in Fig.3, which were determined by the ED and the LS analysis as well as the PRG analysis (see [3–5] for details of the analysis). In both cases, the ID regions are considerably enlarged and the narrow H/LD regions exist near the  $(\Delta, D_4) = (1, 0)$  point (isotropic point). The H/LD region at the larger  $D_4$  case is completely separated from that near the  $(\Delta, D_4) = (1, 0)$  point in (b) and (c), while it does not exist for larger  $D_4$  case in (a). The ID region in (a) survives even in the  $D_4 \rightarrow \infty$  limit, the reason of which will be discussed in §4. The H/LD-ID transition line and the ID-Néel transition line in Figs.3(b) and (c) merge at the multicritical point  $(\Delta, D_4) \simeq (9.5, 8.5)$ . In the upper right region of this multicritical point, there exists the H/LD-Néel transition line.

Kjäll et al. [15] also studied the model (2) and draw the phase diagrams. Since they draw the phase diagrams on the  $D_2 - D_4$  plane for the  $\Delta = 1.0$  and the  $\Delta = 4.5$  cases, we cannot directly compare our phase diagrams with theirs. However, we can compare ours and theirs along some lines, for instance, the  $D_4$  line with  $\Delta = 1.0$  and  $D_2 = 0.0$ . On these lines, our results and theirs are consistent with each other.

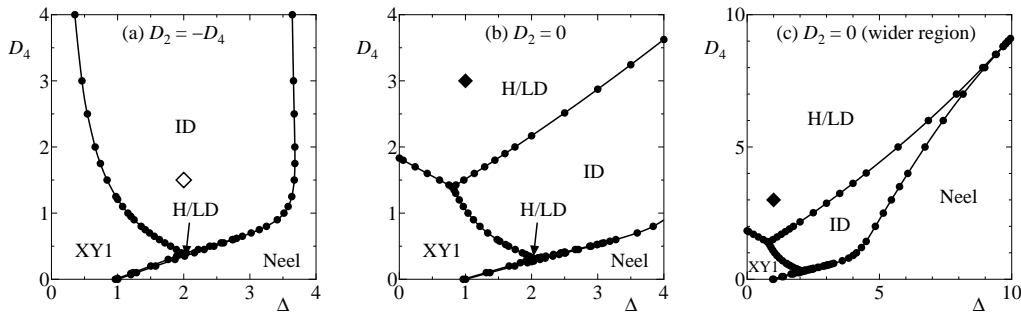


**Fig. 3.** Phase diagram of Hamiltonian (2) on the  $\Delta - D_4$  plane for (a)  $D_2 = -D_4$  and (b), (c)  $D_2 = 0$ . For simplicity, we restrict ourselves to the case of  $\Delta \geq 0$  and  $D_4 \geq 0$ . The open and closed diamond marks ( $\diamond$  and  $\blacklozenge$ ) show the points where the edge mode behaviors are calculated.

## 3. Edge Modes

To investigate the behaviors of the edge modes, we calculated the low-lying excited states by the DMRG under the OBC up to 480 sites at the  $\diamond$  point  $(\Delta, D_2, D_4) = (2, -1.5, 1.5)$  and the  $\blacklozenge$  point

$(\Delta, D_2, D_4) = (1, 0, 3)$  in Fig.3, as representatives of the ID state and the H/LD state, respectively. We calculated finite-size gaps with the  $N$ -spin system defined by

$$\Delta E_{01} \equiv E_0(M=1) - E_0(M=0), \quad \Delta E_{02} \equiv E_0(M=2) - E_0(M=0). \quad (3)$$

Here  $E_0(M=0)$ ,  $E_0(M=1)$  and  $E_0(M=2)$  are the lowest energies within the subspaces  $M=0$ ,  $M=1$  and  $M=2$ , respectively, where  $M \equiv \sum_j S_j^z$  is the total magnetization. We also calculated the local magnetization  $m(j)$  and their sum defined by

$$m(j) = \langle S_j^z \rangle, \quad Q(j) = \sum_{i=1}^j m(i), \quad (4)$$

respectively.

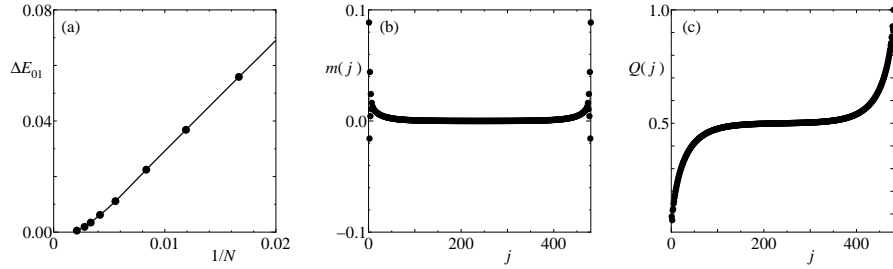


**Fig. 4.** The lowest  $M=1$  mode at the  $\diamond$  point (ID phase)  $(\Delta, D_2, D_4) = (2, -1.5, 1.5)$ .

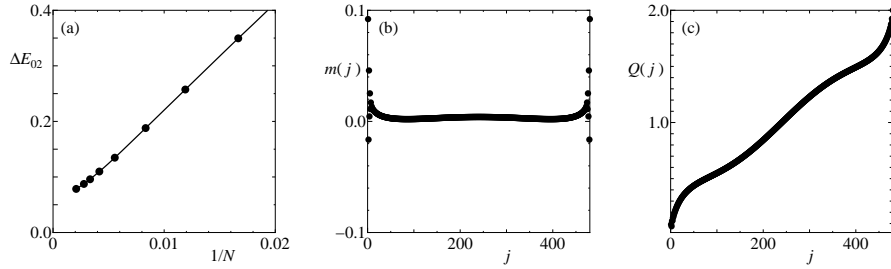


**Fig. 5.** The lowest  $M=2$  mode at the  $\diamond$  point (ID phase)  $(\Delta, D_2, D_4) = (2, -1.5, 1.5)$ .

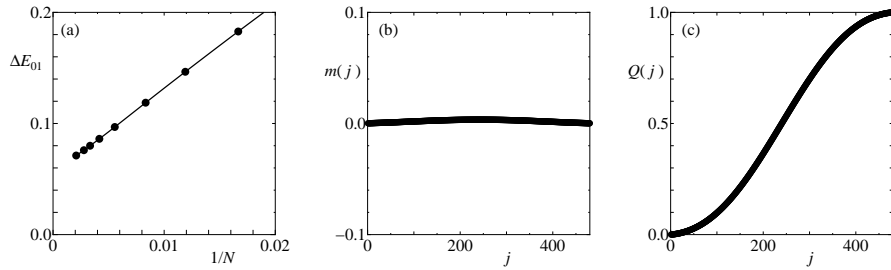


**Fig. 6.** The lowest  $M=1$  mode at the  $\blacklozenge$  point (ID state)  $(\Delta, D_2, D_4) = (1, 0, 3)$ .

We show the results at the  $\diamond$  point (ID state) in Fig.4 (the lowest  $M=1$  mode) and in Fig.5 (the lowest  $M=2$  mode). We can see that the  $M=1$  mode is gapless and an edge-localized mode, while

the  $M = 2$  mode is gapful and a bulk mode. Figure 6 shows the  $M = 1$  mode at the  $\blacklozenge$  point (H/LD state), from which we know that this mode is gapful and a bulk mode. These behavior are consistent with the VBS pictures as will be discussed in §4.

#### 4. Discussion

In Fig.3(a), the ID phase survives even in the  $D_4 \rightarrow \infty$  limit. In the  $D_2 = -D_4$  case, the on-site anisotropy terms can be expressed as  $D_4 \sum_j (S_j^z)^2 [(S_j^z)^2 - 1]$ . Thus, the  $S_j^z = 0$  and  $S_j^z = \pm 1$  states are not affected by the on-site anisotropy terms, while the  $S_j^z = \pm 2$  state is strongly suppressed for larger  $D_4$ . Thus, in the  $D_4 \rightarrow \infty$  case, we can map the present model onto the  $T = 1$  model by neglecting the  $S_j^z = \pm 2$  states, which results in

$$\mathcal{H}_{\text{eff}}^{(1)} = 3 \sum \left( T_j^x T_{j+1}^x + T_j^y T_{j+1}^y + \Delta_{\text{eff}} T_j^z T_{j+1}^z \right), \quad \Delta_{\text{eff}} = \frac{1}{3} \Delta. \quad (5)$$

Here the Haldane state of  $\mathcal{H}_{\text{eff}}^{(1)}$  corresponds to the ID state of the present  $S = 2$  model. The XY-Haldane transition point of  $\mathcal{H}_{\text{eff}}^{(1)}$  is exactly  $\Delta_{\text{eff}} = 0$  [16–20], and the Haldane-Néel transition point is  $\Delta_{\text{eff}} \simeq 1.23$  [21, 22]. These points correspond to  $\Delta = 0$  and  $\Delta \simeq 3.69$  in our  $S = 2$  chain, respectively, which well explains the behaviors of the XY1-ID line and the ID-Néel line in the  $D_4 \rightarrow \infty$  limit of Fig.3(a).

Also in the  $D_2 = 0$  case, the  $S_j^z = \pm 2$  is strongly suppressed for large  $D_4$ . If we project out the  $S_j^z = \pm 2$  states, we obtain

$$\mathcal{H}_{\text{eff}}^{(2)} = 3 \left\{ \sum \left( T_j^x T_{j+1}^x + T_j^y T_{j+1}^y + \Delta_{\text{eff}} T_j^z T_{j+1}^z \right) + D_{2,\text{eff}} \sum_j (S_j^z)^2 \right\}, \quad D_{2,\text{eff}} = \frac{1}{3} D_4. \quad (6)$$

In this case, the Haldane state and the LD state of  $\mathcal{H}_{\text{eff}}^{(2)}$  correspond to the ID state and the LD state of the present  $S = 2$  model, respectively. The multicritical point among the Haldane, LD and Néel phases of  $\mathcal{H}_{\text{eff}}^{(2)}$  is  $(\Delta_{\text{eff}}, D_{2,\text{eff}}) \simeq (3.2, 2.9)$  [22], which reads  $(\Delta, D_4) \simeq (9.4, 8.7)$ . Thus the multicritical point among the ID, LD and Néel phases in Fig.3(c) is well explained.

Figure 7 shows the VBS pictures with edges for the Haldane (H) state, the ID state and the LD state. For the Haldane state, there appear  $S = 1$  edge spins. In the presence of the on-site anisotropy, the  $S^z = \pm 1$  edge states have higher energies than the  $S_z = 0$  state. The lowest  $M = 0$  mode can be made by use of two  $S^z = 0$  edge spins. On the other hand, the lowest  $M = 1$

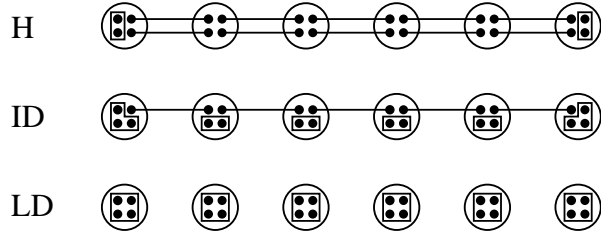


**Fig. 7.** VBS pictures with edges for the Haldane (H) state, the ID state and the LD state.

edge mode consists of the  $S^z = 0$  edge spin and the  $S^z = 1$  edge spin, which means that the  $M = 1$  edge mode is gapful. We note that, in the case of  $D_2 = D_4 = 0$ , we can construct the gapless edge modes with  $M = 1$  and  $M = 2$  without the loss of on-site energy, because  $S_z = 0$  and  $S^z = 1$  edge spins have same energies, as was numerically obtained by Qin et al. [23].

For the ID state, there appear  $S = 3/2$  edge spins. The  $S^z = \pm 1/2$  states have lower energies than the  $S^z = \pm 3/2$  states. The lowest  $M = 0$  mode is constructed by use of an  $S^z = +1/2$  edge spin and an  $S^z = -1/2$  edge spin, while the lowest  $M = 1$  mode by use of two  $S^z = +1/2$  edge spins. Thus, there appears the  $M = 1$  gapless edge mode in the ID phase. Because we have to use an  $S^z = 3/2$  edge state for constructing an  $M = 2$  edge mode, there is no  $M = 2$  gapless edge mode in

the ID phase. Thus the calculated behaviors in Figs.4 and 5 are successfully explained by use of the VBS pictures.

About the LD state, to construct an edge  $M = 1$  mode, it is necessary to change the  $S^z = 0$  state of either edge spin to the  $S^z = 1$  state, which brings about the energy loss of  $D_4$  in the case of  $D_2 = 0$ ,  $D_4 > 0$ . Thus it is clear that the  $M = 1$  mode is gapful, which is consistent with Fig.6.

In conclusion, we have investigated the properties of edge modes in the ID and LD states of the  $S = 2$  quantum spin chain with the  $XXZ$  and the generalized on-site anisotropies. These are well explained by use of the VBS pictures.

## Acknowledgements

We would like to express our appreciation to Masaki Oshikawa for his invaluable discussions and comments as well as for his interest in this study. We are deeply grateful to Frank Pollmann for his stimulating discussions. We also thank the Supercomputer Center, Institute for Solid State Physics, the University of Tokyo, and the Computer Room, Yukawa Institute for Theoretical Physics, Kyoto University. This work was partly supported by Grants-in-Aid (Nos. 23340109 and 23540388) for Scientific Research from the Ministry of Education, Culture, Sports, Science and Technology of Japan.

## References

- [1] F. D. M. Haldane: Phys. Lett. A **93** (1983) 464.
- [2] F. D. M. Haldane: Phys. Rev. Lett. **50** (1983) 1153
- [3] T. Toengawa, K. Okamoto, H. Nakano, T. Sakai, K. Nomura, and M. Kaburagi: J. Phys. Soc. Jpn. **80** (2011) 043001.
- [4] K. Okamoto, T. Tonegawa, H. Nakano, T. Sakai, K. Nomura, and M. Kaburagi: J. Phys. Conf. Ser. **302** (2011) 012014.
- [5] K. Okamoto, T. Tonegawa, H. Nakano, T. Sakai, K. Nomura, and M. Kaburagi: J. Phys. Conf. Ser. **320** (2011) 012018.
- [6] K. Okamoto and K. Nomura: Phys. Lett. A **169** (1992) 433.
- [7] K. Nomura and K. Okamoto: J. Phys. A: Math. Gen. **27** (1994) 5773.
- [8] A. Kitazawa: J. Phys. A **30** (1997) L285.
- [9] K. Nomura and A. Kitazawa: J. Phys. A **31** (1998) 7341.
- [10] M. P. Nightingale: Physica A **83** (1976) 561.
- [11] M. Oshikawa: J. Phys.: Condens. Matter **4** (1992) 7469.
- [12] T. Tonegawa, T. Nakao, and M. Kaburagi: J. Phys. Soc. Jpn. **65** (1996) 3317.
- [13] S. Todo, M. Matsumoto, C. Yasuda, and H. Takayama: Phys. Rev. B **64** (2001) 224412.
- [14] Y.-C. Tzeng: Phys. Rev. B **86** (2012) 024403.
- [15] J. A. Kjäll, M. P. Zaletel, R. S. K. Mong, J. H. Bardarson, and F. Pollmann: Phys. Rev. B **87** (2013) 215106.
- [16] F. C. Alcaraz and A. Moreo: Phys. Rev. B **46** (1992) 2896.
- [17] A. Kitazawa, K. Nomura, and K. Okamoto: Phys. Rev. Lett. **76** (1996) 4038.
- [18] A. Kitazawa and K. Nomura: J. Phys. Soc. Jpn. **66** (1997) 3944.
- [19] K. Nomura and A. Kitazawa: J. Phys.: Math. Gen. **31** (1998) 7341.
- [20] A. Kitazawa, K. Hijii, and K. Nomura: J. Phys.: Math. Gen. **36** (2003) L351.
- [21] T. Sakai and M. Takahashi: J. Phys. Soc. Jpn. **59** (1990) 2688.
- [22] W. Chen, K. Hida, and B. C. Sanctuary: Phys. Rev. B **67** (2003) 104401.
- [23] S. Qin, T.-K. Ng, and Z.-B. Su: Phys. Rev. B **52** (1995) 2844.